Crystalline and vitreous Na3.89Ca0.67Al0.23Ti0.77(PO4)3 : Synthesis, crystal structure, vibrational and UV–Visible spectra

A. Nazih, Saida Krimi, Stanislav Pechev, Matias Velázquez, Michel Couzi, Abdelaziz El Jazouli

Crystalline and vitreous $Na_{3.89}Ca_{0.67}Al_{0.23}Ti_{0.77}(PO_4)_3$: Synthesis, crystal structure, vibrational and UV–Visible spectra

Nazih A.[a], Krimi S.[a], Pechev S.[b], Velázquez M.[c], Couzi M.[d], El Jazouli A.[e]

[a] *Materials Engineering for Environment and Valorization Laboratory (GeMEV), MCC Team, Faculty of Science Ain Chock, Hassan II University of Casablanca, Morocco*
[b] *Univ. Bordeaux, CNRS, Bordeaux INP, ICMCB UMR 5026, F-33600 Pessac, France*
[c] *Univ. Grenoble Alpes, CNRS, Grenoble INP, SIMAP 38000 Grenoble, France*
[d] *Univ. Bordeaux, CNRS, ISM UMR 5255, 351 Cours de la Libération, F-33405 Talence Cedex, France*
[e] *Faculty of Science Ben M'Sik, Hassan II University of Casablanca, Morocco*

Abstract : $Na_{3.89}Ca_{0.67}Al_{0.23}Ti_{0.77}(PO_4)_3$ phosphate exists in both crystalline and vitreous forms. It has been synthesized as microcrystalline powder, single crystals and glass. The structure of the crystalline form, belonging to Nasicon family with $M(1)M(2)_3A_2(PO_4)_3$ formula, was solved by single crystal X-ray diffraction (Space group R32, Z = 6, a_h = 8.9976(1) Å, c_h = 21.8312(3) Å, R_1 = 0.03, wR_2 = 0.06). A Rietveld refinement was also performed. The structure is formed by a 3D network of PO_4 tetrahedra and AO_6 (*A*= Na/Ca and Al/Ti) octahedra sharing corners. One of the two positions of A sites is statistically occupied by Na^+ and Ca^{2+}, the other position is statistically occupied by Al^{3+} and Ti^{4+}. The remaining sodium atoms occupy totally M(1) and partially M(2) interstitial sites. Raman and infrared spectra show for the crystalline powder, broad peaks attributed principally to monophosphate PO_4 modes. The structure of the glass contains PO_4 and P_2O_7 groups and short -Ti-O-Ti-O- chains. UV–Visible spectra consist of strong bands at high energy assigned to O-Ti and O-Al electronic charge transfers.

Keywords : NaCaAlTiPO-phosphate ; Nasicon ; Nasiglass ; Structure ; Raman ; Infrared ; UV–Visible

1. Introduction

Nasicon-type materials (Nasicon: Na super ionic conductors) have been extensively studied after the discovery of sodium super ionic conductors $Na_{1+x}Zr_2Si_xP_{3-x}O_{12}$ by Goodenough et al. [1]. These materials were known to show relatively high chemical stability and have been proposed for use in various fields of solid-state chemistry: solid electrolytes, electrode materials, low thermal expansion ceramics, ionic conductors, sensors, catalysts, luminophores and materials for immobilization of radioactive waste [2–14]. Their structure was first described for $NaA_2(PO_4)_3$ (*A* = Ti, Ge, Zr) phosphates [15]. It consists of a three-dimensional framework built up of PO_4 tetrahedra sharing corners with AO_6 octahedra. Within this covalent skeleton, there are two sites, labelled M(1) and M(2). There are three M(2) sites and one M(1) site by formula unit: $M(1)M(2)_3A_2(PO_4)_3$. The M(1) site, fully occupied by sodium, is an antiprism formed by the triangular faces of two AO_6 octahedra along c axis of the hexagonal cell. Thus, the network of $NaA_2(PO_4)_3$ (*A* = Ti, Ge, Zr) phosphates can be considered as made up of infinite ribbons of composition $[O_3AO_3NaM(1)O_3AO_3{-}O_3AO_3NaM(1)O_3AO_3]_\infty$ connected by PO_4 tetrahedra. The M(2) sites, totally empty in $NaA_2(PO_4)_3$ (*A* = Ti, Ge, Zr), are located between these ribbons in large cavities with an eight-fold coordination. M(1) and M(2) sites can be completely empty like in $NbTi(PO_4)_3$ [16] and $Al_{0.5}Nb_{1.5}(PO_4)_3$ [17], partially occupied like in $M_{0.5}Ti_2(PO_4)_3$ (M = Ca, Mn, Fe, Co, Pb) [18–25], $Ba_{0.5}FeNb(PO_4)_3$ [26], $NaA_2(PO_4)_3$ (*A* = Ti, Ge, Zr) [15], $Li_3Ti_2(PO_4)_3$ [27], $Na_3AZr(PO_4)_3$ (*A* = Mg, Ni) [28], $Na_{3.5}Cr_{1.5}Co_{0.5}(PO_4)_3$ [29] and $Na_2FeA(PO_4)_3$ (*A* = Ti, Sn) [30,31] or full as in $Na_5A(PO_4)_3$ (*A* = Ti, Zr) [32–33] and $Na_4AB(PO_4)_3$ (*A* = Mg, Mn, Ni; *B* = Al, Cr) [34–36]. Nasicon structure permits a large number of substitutions at M(1), M(2), A and P sites giving rise to a range of compositions. It can accommodate several ions with different sizes and charges [37]. Previous studies showed that introduction of Al^{3+} ions in Nasicon-type phosphates improves their ionic conductivity [38–40]. Some compositions of Nasicon type materials can be obtained in the glassy form like $Na_{5-2x}Ca_xTi(PO_4)_3$ ($0 \le x \le 1$) and $Na_3Ca_{1-x}Mn_xTi(PO_4)_3$ ($0 \le x \le 1$) [41–43]. They are called Nasiglasses (Sodium superionic conductor glasses). During the study of $Na_{3+2x+y}Ca_{1-x}Al_yTi_{1-y}(PO_4)_3$ system, we isolated a new composition (x = 0.33, y = 0.27: $Na_{3.89}Ca_{0.67}Al_{0.23}Ti_{0.77}(PO_4)_3$) which exists in both crystalline and vitreous forms. We present here its synthesis

* Corresponding author.
E-mail address: saida.krimi@univh2c.ma (S. Krimi).

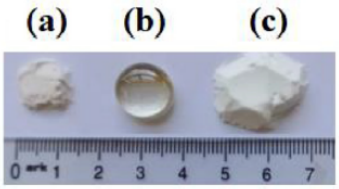

Fig. 1. Photographs of (a) grinded glass, (b) glass block and (c) crystallized powder of $Na_{3.89}Ca_{0.67}Al_{0.23}Ti_{0.77}(PO_4)_3$ samples.

methods, crystal structure determination by single crystal X-ray diffraction (SCXRD) and powder X-ray diffraction (PXRD), as well as its vibrational and optical spectra.

2. Experimental

2.1. Synthesis

$Na_{3.89}Ca_{0.67}Al_{0.23}Ti_{0.77}(PO_4)_3$ was obtained as single crystal, microcrystalline powder and glass. The starting reagents used for the synthesis were Na_2CO_3 (99.5%), $CaCO_3$ (99%), Al_2O_3 (99%), TiO_2 (99.5%) and $(NH_4)_2HPO_4$ (99%). Single crystals were prepared by melting in a platinum crucible the mixture of reagents, (Atomic ratios: Na/Ca/Ti/Al/P: 7/2/1/1/6) at 1000 °C, followed by slow cooling at rate of 5 °C/h, until 250 °C and finally cooled to room temperature by turning off the furnace power (Amount of final compound: about 5 g). The crystals are transparent and colorless. White microcrystalline powder of $Na_{3.89}Ca_{0.67}Al_{0.23}Ti_{0.77}(PO_4)_3$ was obtained by standard solid-state preparation, according to the following reaction:

$$\frac{3.89}{2}Na_2CO_3 + 0.67CaCO_3 + \frac{0.23}{2}Al_2O_3 + 0.77TiO_2 + 3(NH_4)_2HPO_4 \downarrow$$
$$Na_{3.89}Ca_{0.67}Al_{0.23}Ti_{0.77}(PO_4)_3 + 6NH_3 + \frac{9}{2}H_2O + \frac{5.23}{2}CO_2$$

Stoichiometric proportions of reagents, in order to obtain 1 g of the final compound, are heated respectively at 200 °C (12 h), 400 °C (12 h) and 700 °C (24 h) with intermediate grindings. Crystalline powder of $Na_{3.89}Ca_{0.67}Al_{0.23}Ti_{0.77}(PO_4)_3$ can also be obtained by recrystallization of the corresponding glass at 650 °C for 24 h. The glass was obtained in air by melting, in a platinum crucible, stochiometric amounts of reagents (about 10 g). In a first step, powder was heated at 200 °C (12 h), 400 °C (6 h) and 600 °C (4 h) to eliminate NH_3, H_2O and CO_2gasses. The temperature was then progressively raised to 1050 °C and held constant at this value for 15 min. The liquid was then poured onto a metal plate. Under these conditions, the glass is colorless (Fig.1(b)). The amorphous state of the vitreous sample was confirmed by powder X-ray diffraction (Fig. 2(b)). No Bragg peaks were detected in a wide range of 2θ angles between 10° and 80° We observed only a broad peak around 2θ = 32° characteristic of amorphous compounds. The glass was also characterized by density measurement (d = 2.73) and DTA (Fig. 3). The values of the glass transition and crystallization temperatures are T_g = 436 °C and T_c = 589 °C. Chemical analysis was performed, for all elements except oxygen, by inductively coupled plasma-optical emission spectroscopy (ICP-OES) using an ICAP 7000 (Thermo Fisher) spectrometer. The number of oxygen is deduced from the balance of positive and negative charges. The analysis results led to the formula $Na_{3.90}Ca_{0.71}Al_{0.25}Ti_{0.75}P_{2.98}O_{11.985}$ which is close to the studied one ($Na_{3.89}Ca_{0.67}Al_{0.23}Ti_{0.77}P_3O_{12}$), taking into account the measurement error (± 0.03).

2.2. Single crystal and powder X-ray diffraction

A platelet shaped $Na_{3.89}Ca_{0.67}Al_{0.23}Ti_{0.77}(PO_4)_3$ colorless single crystal (0.34×0.191×0.041 mm^3) has been selected and mounted on glass fiber for X-ray diffraction analysis. The diffraction data were collected on a Nonius Kappa CCD diffractometer with a graphite monochromator using MoKα radiation. The single crystal data and the conditions of data collection are summarized in Table 1. The powder of $Na_{3.89}Ca_{0.67}Al_{0.23}Ti_{0.77}(PO_4)_3$ was analyzed by X-ray diffraction with a Panalytical X'Pert θ–2θ (CuKα1.2 radiation) diffractometer. Its pattern (Fig. 2(a)) shows a Nasicon-type phase and some very weak lines attributed to rutile TiO_2 [ASTM powder diffraction data file, N°01–087–0710] and $Na_4P_2O_7$ [ASTM powder diffraction data file, N°00–010–0187]. Results of powder Rietveld refinement of $Na_{3.89}Ca_{0.67}Al_{0.23}Ti_{0.77}(PO_4)_3$ are reported in Table 2.

Table 1
Results of single crystal refinement of $Na_{3.89}Ca_{0.67}Al_{0.23}Ti_{0.77}(PO_4)_3$.

Chemical formula	$Na_{3.89}Ca_{0.67}Al_{0.23}Ti_{0.77}(PO_4)_3$
Temperature	293(2) K
Wavelength	0.71073 Å
Crystal system / Space group	Trigonal / R32 (155)
Unit cell dimensions (Å)	a = b = 8.9976 (1), c = 21.8312 (3) $\alpha = \beta = 90°$, $\gamma = 120°$
Volume / Z	1530.6 (3) $Å^3$ / 6
Molecular weight (g/mol)	444.28
Density (calculated)	2.892 g/cm^3
Absorption coefficient	1.733 mm^{-1}
F(000)	1302.7
Crystal size	0.34 × 0.191 × 0.041 mm^3
Theta range for data collection	3.21 to 33.62°
Index ranges	-13≤h≤14 / -13≤k≤13 / -33≤l≤33
Reflections collected	6991
Independent reflections	1329 [R(int) = 0.0297]
Completeness to theta = 33.62°	98.9 %
Refinement method	Full-matrix least-squares on F^2
Data / restraints / parameters	1329/ 3/ 72
Goodness-of-fit on F^2	1.089
Final R indices [I>2sigma(I)]	R_1 = 0.0268, wR_2 = 0.0600
R indices (all data)	R_1 = 0.0304, wR_2 = 0.0643
Absolute structure parameter	0.00(5)
Extinction coefficient	0.0020(2)
Largest diff. peak and hole	0.613 (Na2) and -0.651(Na2) e.$Å^{-3}$

Table 2
Results of powder Rietveld refinement of $Na_{3.89}Ca_{0.67}Al_{0.23}Ti_{0.77}(PO_4)_3$.

Structural formula	$Na_{3.89}Ca_{0.67}Al_{0.23}Ti_{0.77}(PO_4)_3$
Wavelength (Å)	$\lambda_{K\alpha1}$=1.5406; $\lambda_{K\alpha2}$= 1.5444
Step width (2θ°); angular range (°)	0.02; 8-80
Program	Fullprof
Zero point (2θ°)	0.0304(16)
Pseudo-Voigt function PV = ηL +(1-η)G	η = 0.2862(437)
Half-width parameters: U; V; W	0.16(2); -0.07(1); 0.02 (2)
Number of reflections	2827
System; space group; Z; Density (calculated)	Hexagonal; R32; 6; 2.902 g/cm^3
a (Å); c (Å); V ($Å^3$)	8.9906 (4); 21.8096(1); 1526.7(2)
R_B; R_F; R_P; R_{WP}	3.12%; 2.99%; 7.27%; 10.1%
χ^2	1.58

2.3. Vibrational and reflectance diffusion spectroscopies

Infrared spectra of a mixture of KBr and $Na_{3.89}Ca_{0.67}Al_{0.23}Ti_{0.77}(PO_4)_3$ (3%) powders were recorded by the diffuse reflection technique using a Bruker IFS Equinox 55 FTIR spectrometer in the range of 1400 – 400 cm^{-1}. Raman spectra were recorded under the microscope of a Dilor XY multichannel spectrometer in the range of 1500 – 150 cm^{-1}. Excitation was accomplished with 514.5 nm line of argon-ion laser. The diffuse

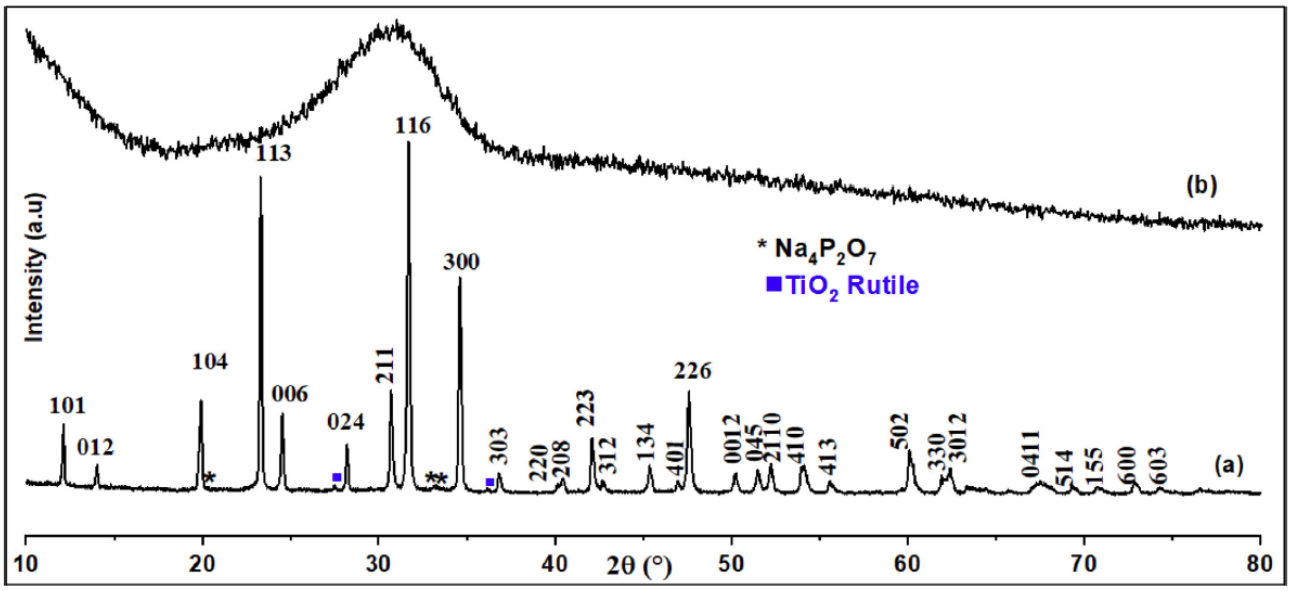

Fig. 2. Powder X-ray diffraction, at room temperature, of (a) crystalline and (b) vitreous forms of $Na_{3.89}Ca_{0.67}Al_{0.23}Ti_{0.77}(PO_4)_3$.

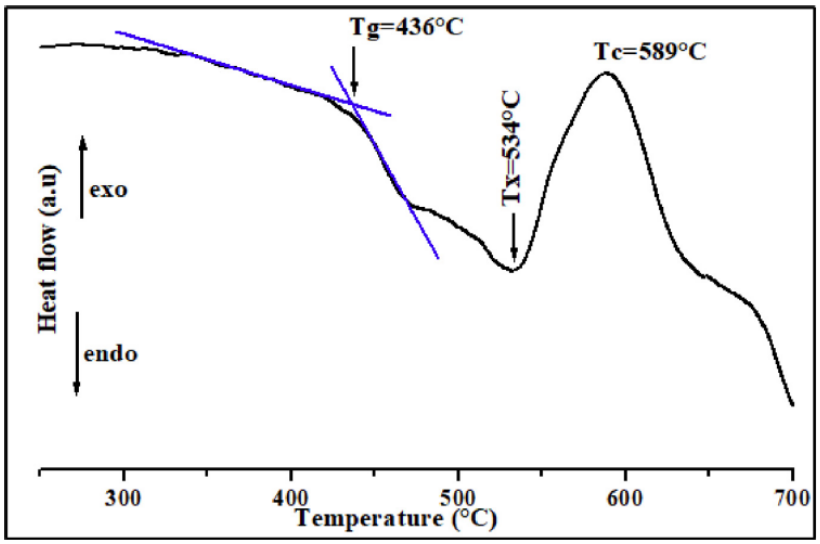

Fig. 3. DTA curve of vitreous $Na_{3.89}Ca_{0.67}Al_{0.23}Ti_{0.77}(PO_4)_3$.

reflectance spectra were recorded in the range 200 – 1400 nm at room temperature using a Cary 5000 spectrophotometer (Varian).

3. Results and discussion

3.1. Single crystal structure resolution of $Na_{3.89}Ca_{0.67}Al_{0.23}Ti_{0.77}(PO_4)_3$

The structure of $Na_{3.89}Ca_{0.67}Al_{0.23}Ti_{0.77}(PO_4)_3$ was solved using single crystal X-ray diffraction data. The observed reflection conditions agree with the R32 space group. The starting model was established by direct methods using SHELXS-97 program [44]. The refinement with anisotropic displacement parameters for all atoms converged to $R_1 = 0.0304$, $wR_2 = 0.0643$ for 72 refined parameters based on 1329 observed reflections. The peaks of the residual electronic density map were in the range between 0.613 and −0.651 e$Å^{-3}$. The final atomic coordinates with the equivalent isotropic displacement parameters are presented in Table 3. Selected interatomic distances, bond valences and angles are listed in Tables 4. Bond valence sums are calculated using the Brown method [45]: Vi = SjVij, where Vij = exp[(Rij - *dij*)/*b*], *b* = 0.37 Å, Rij (Å) characterizing a cation–anion pair (O^{2-}: 1.815 for Ti^{4+}, 1.651 for Al^{3+}, 1.967 for Ca^{2+}, 1.803 for Na^{+} and 1.617 for P^{5+}) and dij: distance between i and j atoms. Anisotropic displacement parameters for $Na_{3.89}Ca_{0.67}Al_{0.23}Ti_{0.77}(PO_4)_3$ are reported in Table 5.

3.2. Rietveld refinement of $Na_{3.89}Ca_{0.67}Al_{0.23}Ti_{0.77}(PO_4)_3$

The structure of $Na_{3.89}Ca_{0.67}Al_{0.23}Ti_{0.77}(PO_4)_3$ has been also determined from powder X-ray diffraction data by the Rietveld method [46], using the FullPof program [47]. The initial atomic coordinates used for the refinement were those obtained previ-

Table 3
Atomic coordinates, occupancy rate and equivalent isotropic displacement parameters of $Na_{3.89}Ca_{0.67}Al_{0.23}Ti_{0.77}(PO_4)_3$ obtained from single crystal and powder X-ray diffraction (underlined).

Atom	Wyckoff site	x	y	z	Occupation	Ueq (Å2)/ Biso
Al/Ti	6c	0	0	0.1009(1)	0.23(1)/ 0.77(1)	0.008(1)
		0	0	0.1011(5)	0.23/ 0.77	1.84(26)
Na1/ Ca	6c	1/3	-1/3	0.0697(1)	0.33(1)/0.67(1)	0.017(1)
		1/3	-1/3	0.0692(5)	0.33/0.67	0.96(27)
Na2	6c	0	0	0.2489(1)	1	0.042(1)
		0	0	0.2505(9)	1	2.30(33)
Na3	9d	-0.6176(2)	0	0	1	0.032(1)
		-0.6154(13)	0	0	1	2.06(35)
Na4	9e	1/3	0.3318(3)	1/6	0.71(1)	0.050(1)
		1/3	0.3363(13)	1/6	0.71	0.98(50)
P1	9d	-0.2800(1)	0	0	1	0.010(1)
		-0.2782(5)	0	0	1	0.36(21)
P2	9e	1/3	-0.0092(1)	1/6	1	0.012(1)
		1/3	-0.0072(5)	1/6	1	1.34(26)
O1	18f	0.1779(2)	0.0173(2)	0.1566(1)	1	0.019(1)
		0.1773(10)	0.0162(16)	0.1580(5)	1	1.07(13)
O2	18f	0.3746(3)	-0.0812(3)	0.1108(1)	1	0.039(1)
		0.3827(13)	-0.0832(13)	0.1142(4)	1	1.07(13)
O3	18f	-0.2946(2)		0.0077(1)	1	0.017(1)
		-0.2962(13)	0.1601(2)	0.0064(5)	1	1.07(13)
O4	18f	-0.1898(3)	0.1618(9)	0.0562(1)	1	0.033(1)
		-0.1941(10)	-0.0241(3)	0.0565(3)	1	1.07(13)
			-0.0230(12)			

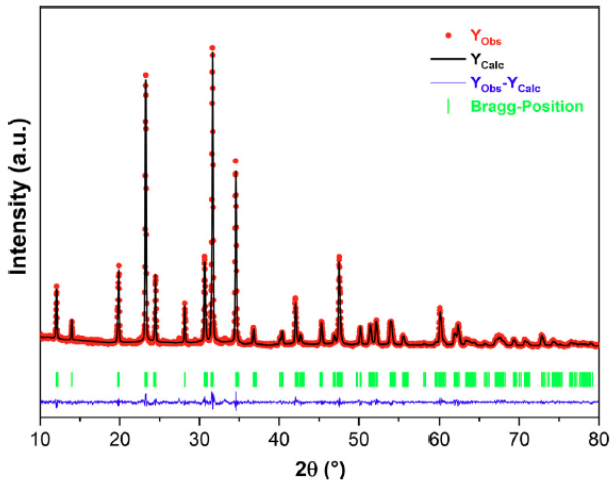

Fig. 4. Observed (...), calculated (—), difference (—) and Bragg position (|) for powder X-ray diffraction patterns of $Na_{3.89}Ca_{0.67}Al_{0.23}Ti_{0.77}(PO_4)_3$.

ously from single crystal X-ray diffraction study. Experimental conditions and results of the refinement are reported in Tables 2 4. The refinement led to a good agreement between the experimental and calculated PXRD patterns (Fig. 4) and to good reliability factors (Table 2). All the observed reflections could be indexed in the space group R32 (Table 6).

3.3. *Structure description*

$Na_{3.89}Ca_{0.67}Al_{0.23}Ti_{0.77}(PO_4)_3$ crystallizes in the trigonal space group R32. Its structure consists of a 3D network of PO_4 tetrahedra and AO_6 [A = Na/Ca; Al/Ti] octahedra sharing corners (Fig 5). One of the two positions of A sites is statistically occupied by Na^+ (Na1) and Ca^{2+} ions, the other position is statistically shared by Al^{3+} and Ti^{4+} ions, the remaining sodium ions fully occupy the M(1) site and partially the M(2) sites: $[Na]_{M1}[Na_{2.56}]_{M2}[Na_{0.33}Ca_{0.67}Al_{0.23}Ti_{0.77}]_A(PO_4)_3$. The M(1) site is an antiprism formed by the triangular faces of Na/CaO_6 and Al/TiO_6 octahedra along c-axis of the hexagonal cell. The structure can be described as infinite ribbons $([Na1/CaO_6][Na1/CaO_6][Na2O_6(M1)][Al/TiO_6][Al/TiO_6])_\infty$ parallel to the [001] direction and linked by PO_4 tetrahedra in the three directions (Fig. 5). The M(2) sites are located between these ribbons. The 2–2 cationic ordering in the A sites creates two different M(2) sites (Na3: 9d; Na4: 9e) and two different PO_4 groups (P1: 9d; P2: 9e). The M(1) site, occupied by sodium, Na2 (6c position) is surrounded by three O3 oxygens belonging to one face of $Na1/CaO_6$ octahedron and three O1 oxygens belonging to one face of Al/TiO_6 octahedron (Fig. 6). The Na2 – O3 distances (2.429 Å), where O3 is connected to Na1/Ca, are shorter than Na2 – O1 distances (2.530 Å), where O1 is linked to Al/Ti; Al/Ti atoms are slightly displaced from the geometrical center of the octahedron due to the repulsions of oxygen O4 planes along the c axis (Figs. 5 and 7) implying the formation of three short Al/Ti – O4 bonds (1.882 Å) and three long Al/Ti–O1 bonds (1.954 Å) (Fig. 6). The average distance, <Al/Ti - O> ≈ 1.918 Å is shorter than the calculated one (1.99 Å) from ionic radii of Al^{3+}, Ti^{4+} and O^{2-} [48]. The $Na1/CaO_6$ octahedron is distorted (Fig. 6), Na1/Ca – O2 distances (2.290 Å) are shorter than the Na1/Ca – O3 distances (2.439 Å) due to the repulsions between O2 oxygen planes (Fig. 7). Along the c axis, the Al/Ti – Al/Ti distance (4.40 Å) is longer than the Na1/Ca – Na1/Ca distance (4.26 Å) because the Al^{3+}/Ti^{4+} – Al^{3+}/Ti^{4+} electrostatic repulsions are more important than the Na^+/Ca^{2+} – Na^+/Ca^{2+}repulsions (Fig. 7). The Na3 and Na4 sodium atoms occupy two types of M(2) sites (9d and 9e positions) (Fig. 6). Na3 sodium, occupying 9d position of M(2) site, is surrounded by 6 oxygen atoms. The Na3 – O distance range is between 2.398 Å and 2.522 Å. The average distance 2.479 Å is slightly larger than the sum of the ionic radii (r_{Na+}= 1.02 Å; r_{O2-} = 1.40 Å) (Fig. 6). Na4 sodium, occupying 9e position of M(2) site, is surrounded by 8 oxygen atoms with a broad distribution of Na4 – O distances (2.461; 2.656; 2.741; 2.793 Å). In PO_4 tetrahedra, the P – O distances are between 1.513 Å and 1.547 Å. They are similar to those usually found in Nasicon-type phosphates [15,32]. The calculated bond valence (BV) using Brown and Altermatt model [45] are 1.84 for Na1/Ca (expected 1.67), 4.19 for Ti/Al (expected 3.77), 0.97, 0.98 and 0.83 for Na2, Na3

Table 4
Bond lengths (Å), bond valences (BV) and angles (°) for $Na_{3.89}Ca_{0.67}Al_{0.23}Ti_{0.77}(PO_4)_3$ obtained from single crystal and powder X-ray diffraction (underlined).

Bond	length		BV		Angles			
Al/Ti -O4#1	1.882(2)	1.917(8)	< Al/Ti >		$O4^{\#1\#2}$- Al/Ti -$O4^{/\#2}$	×3	95.59(9)	96.5(8)
Al/Ti -O4#2	1.882(2)	1.917(8)	0.765	0.696	$O1^{/\#2}$- Al/Ti -$O1^{\#1\#2}$	×3	85.31(8)	84.4(2)
Al/Ti -O4	1.882(2)	1.917(8)	0.765	0.696	$O4^{/\#1\#2}$- Al/Ti -$O1^{/\#1\#2}$	×3	88.36(8)	88.3(8)
Al/Ti -O1	1.954(2)	1.967(2)	0.765	0.696	$O4^{/\#1\#2}$- Al/Ti -$O1^{/\#1\#2}$	×3	90.28(9)	90.1(7)
Al/Ti -O1#2	1.954(2)	1.967(2)	0.631	0.608	$O4^{/\#1\#2}$- Al/Ti -$O1^{/\#1\#2}$	×3	172.56(9)	171.3(8)
Al/Ti-O1#1	1.954(2)	1.967(2)	0.631	0.608				
Average	**<1.918>**	**<1.942>**	0.631	0.608				
			Σs=4.19	**Σs=3.91**				
Na1/Ca -O2#4	2.290(2)	2.285(1)	< Na1/Ca >		$O2^{/\#4}$-Na1/Ca-$O2^{/\#5}$	×3	105.68(8)	102.9(6)
Na1/Ca -O2	2.290(2)	2.285(1)	0.368	0.369	$O3^{\#6\#7}$- Na1/Ca -$O3^{\#7\#8}$	×3	77.29(6)	77.7(7)
Na1/Ca -O2#5	2.290(2)	2.285(1)	0.368	0.369	$O2^{/\#4\#5}$- Na1/Ca-$O3^{\#6\#7\#8}$	×3	85.89(7)	87.6(6)
Na1/Ca -O3#6	2.4395(2)	2.392(2)	0.368	0.369	$O2^{/\#4\#5}$- Na1/Ca -$O3^{\#6\#7\#8}$	×3	87.17(7)	88.9(7)
Na1/Ca -O3#7	2.4395(2)	2.392(2)	0.246	0.279	$O2^{/\#4\#5}$- Na1/Ca -$O3^{\#6\#7\#8}$	×3	159.16(8)	161.8(7)
Na1/Ca -O3#8	2.4395(2)	2.392(2)	0.246	0.279				
Average	**<2.365>**	**<2.339>**	0.246	0.279				
			Σs=1.84	**Σs=1.94**				
P1-O3	1.520(2)	1.513(9)	1.300	1.325	O3- P1-O(3)#25		111.85(2)	110.7(7)
P1-O3#25	1.520(2)	1.513(9)	1.300	1.325	O3#25- P1-O(4)#25		110.22(10)	110.4(8)
P1-O4	1.545(2)	1.548(1)	1.216	1.205	O3- P1-O4		110.21(1)	110.4(11)
P1-O4#25	1.545(2)	1.548(1)	1.216	1.205	O3#25- P1-O4		108.78(9)	107.7(9)
Average	**<1.533>**	**<1.531>**	**Σs=5.03**	**Σs=5.1**	O4- P1-O4#25		106.90(2)	109.9(8)
					O3- P1-O(4)#25		108.78(9)	107.7(11)
P2-O2#27	1.513(2)	1.508(1)	1.325	1.343	O1- P2-$O1^{\#27}$		105.43(2)	106.9(9)
P2-O2	1.513(2)	1.508(1)	1.325	1.343	$O2^{\#27}$- P2-O2		113.1(2)	106.3(10)
P2-O1	1.547(2)	1.531(2)	1.207	1.262	$O2^{\#27}$- P2-O1		106.38(2)	104.4(11)
P2-O1#27	1.547(2)	1.531(2)	1.207	1.262	O2- P2-O1		112.68(1)	117.7(11)
Average	**<1.530>**	**<1.520>**	**Σs=5.06**	**Σs=5.2**	O2#27- P2-O1#27		112.68(10)	117.7(14)
					O2- P2-O1#27		106.39(12)	104.4(14)
Na2-O3#14	2.428(2)	2.405(18)	0.185	0.194	$O1^{\#2\#1}$- Na2-$O1^{/\#1}$	× 3	63.12(7)	63.0(8)
Na2-O3#15	2.429(2)	2.405(18)	0.184	0.194	$O3^{\#14\#15}$-Na2-$O3^{\#15\#16}$	× 3	77.70(7)	77.2(6)
Na2-O3#16	2.429(2)	2.405(18)	0.184	0.194	$O3^{\#14\#15\#16}$- Na2-$O1^{/\#1\#2}$	× 3	103.89(5)	104.4(8)
Na2-O1#2	2.530(2)	2.530(19)	0.140	0.140	$O3^{\#14\#15\#16}$- Na2-$O1^{/\#1\#2}$	× 3	115.82(5)	115.8(8)
Na2-O1#1	2.530(2)	2.530(19)	0.140	0.140	$O3^{\#14\#15\#16}$-Na2-$O1^{/\#1\#2}$	× 3	166.47(7)	166.9(10)
Na2-O1	2.530(2)	2.530(19)	0.140	0.140				
Average	**<2.479>**	**<2.468>**	**Σs=0.97**	**Σs=1.00**				
Na3-O3#21	2.398(2)	2.406(9)	0.200	0.196	$O3^{\#25}$- Na3-O3		59.88(7)	61.2(5)
Na3-O3#22	2.399(2)	2.406(9)	0.200	0.196	$O3^{\#21\#22}$- Na3-$O3^{/\#25}$	× 2	76.46(7)	75.6(6)
Na3-O2#23	2.517(3)	2.489(14)	0.145	0.157	$O3^{\#21\#22}$- Na3-$O3^{/\#25}$	× 2	136.22(5)	136.8(6)
Na3-O2#24	2.517(3)	2.489(14)	0.145	0.157	$O3^{\#21}$- Na3-$O3^{\#22}$		147.29(1)	147.6(5)
Na3-O3#25	2.522(2)	2.598(9)	0.143	0.117	$O2^{\#23\#24}$- Na3-$O3^{/\#25}$	× 2	80.70(6	79.0(6)
Na3-O3	2.523(2)	2.598(9)	0.143	0.117	$O3^{\#21\#22}$- Na3-$O2^{\#23\#24}$	× 2	81.95(6)	81.7(5)
Average	**<2.479>**	**<2.498>**	**Σs= 0.98**	**Σs= 0.94**	$O2^{\#23\#24}$- Na3-$O3^{/\#25}$	× 2	87.63(7)	87.4(6)
					$O3^{\#21\#22}$- Na3-$O2^{\#23\#24}$	× 2	101.89(6)	102.8(6)
					$O2^{\#23}$- Na3-$O2^{\#24}$		166.54(2)	164.2(6)
Na4-O1#27	2.461(3)	2.500(16)	0.169	0.152	O1#27- Na4-O1		60.04(9)	58.9(6)
Na4-O1	2.461(3)	2.500(16)	0.169	0.152	$O1^{/\#27}$-Na4-$O1^{\#1\#30}$	×2	60.92(7)	60.6(6)
Na4-O2#28	2.656(3)	2.529(12)	0.100	0.141	$O1^{\#30}$-Na4-$O1^{\#1}$		178.45(12)	179.8(5)
Na4-O2#29	2.656(3)	2.529(12)	0.100	0.141	$O1^{/\#27}$-Na4-$O1^{\#1\#30}$	×2	120.63(8)	119.3(6)
Na4-O1#30	2.741(2)	2.728(8)	0.079	0.082	$O2^{\#28}$- Na4-$O2^{\#29}$		100.81(2)	100.1(6)
Na4-O1#1	2.741(2)	2.728(8)	0.079	0.082	$O4^{\#15}$- Na4-$O4^{\#2}$		158.40(2)	157.1(4)
Na4-O4#15	2.793(2)	2.770(7)	0.069	0.073	$O1^{/\#27}$- Na4-$O2^{\#28\#29}$	×2	144.61(8)	145.7(8)
Na4-O4#2	2.793(2)	2.770(7)	0.069	0.073	$O1^{/\#27}$- Na4-$O2^{\#28\#29}$	×2	106.77(7)	107.0(9)
Average	**<2.663>**	**<2.632>**	**Σs= 0.83**	**Σs=0.9**	$O2^{\#28\#29}$- Na4-$O1^{\#1\#30}$	×2	124.82(8)	125.9(5)
					$O2^{\#28\#29}$- Na4-$O1^{\#1\#30}$	×2	53.97(5)	54.2(5)
					$O(1)^{\#1\#30}$-Na(4)-$O(4)^{\#2\#15}$	×2	57.78(5)	59.0(3)
					$O1^{/\#27}$- Na4-$O4^{\#2\#15}$	×2	98.35(9)	96.6(6)
					$O1^{\#1\#30}$- Na4-$O4^{\#2\#15}$	×2	122.56(5)	121.0(5)
					$O1^{/\#27}$- Na4-$O4^{\#2\#15}$	×2	61.98(6)	62.6(5)
					$O2^{\#28\#29}$- Na4-$O4^{\#2\#15}$	×2	90.68(6)	91.0(5)
					$O2^{\#28\#29}$- Na4-$O4^{\#2\#15}$	×2	103.12(6)	103.8(5)

Symmetry transformations used to generate equivalent atoms:
#1 -y,x-y,z; #2 -x+y,-x,z; #3 y-1/3,x-2/3,-z+1/3; #4 -x+y+1,-x,z; #5 -y,x-y-1,z; #6 -x,-x+y-1,-z; #7 x-y+1,-y,-z; #8 y,x,-z; #9 -x+y,-x-1,z; #10 x+1,y,z; #11 x+1/3,y-1/3,z-1/3; #12 x,y-1,z #13 -y+1,x-y,z; #14 -x-1/3,-x+y-2/3,-z+1/3; #15 x-y+2/3,-y+1/3,-z+1/3; #16 y-1/3,x+1/3,-z+1/3; #17 -x+y-1/3,-x-2/3,z+1/3; #18 -y-1/3,x-y+1/3,z+1/3; #19 x+2/3,y+1/3,z+1/3; #20 x-1/3,y+1/3,z+1/3; #21 y-1,x,-z; #22 -x+y-1,-x,z; #23 x-1,y,z, #24 x-y-1.-y.-z; #25 x-y.-y.-z; #26 -y-1.x-y.z; #27 -x+2/3.-x+y+1/3.-z+1/3; #28 -x+y+1.-x+1.z; #29 x-y-1/3.-y+1/3.-z+1/3

Table 5
Anisotropic displacement parameters (Å^2) for $Na_{3.89}Ca_{0.67}Al_{0.23}Ti_{0.77}(PO_4)_3$ (single crystal).

Atom	U^{11}	U^{22}	U^{33}	U^{23}	U^{13}	U^{12}
Al/Ti	0.007(1)	0.007(1)	0.009(1)	0	0	0.004(1)
Na1/Ca	0.018(1)	0.018(1)	0.014(1)	0	0	0.009(1)
Na2	0.056(1)	0.056(1)	0.016(1)	0	0	0.028(1)
Na3	0.019(1)	0.016(1)	0.060(1)	-0.005(1)	-0.002(1)	0.008(1)
Na4	0.018(1)	0.019(1)	0.112(3)	-0.005(1)	-0.009(1)	0.009(1)
P1	0.007(1)	0.008(1)	0.015(1)	0.003(1)	0.001(1)	0.004(1)
P2	0.008(1)	0.009(1)	0.020(1)	-0.001(1)	-0.003(1)	0.004(1)
O1	0.014(1)	0.026(1)	0.022(1)	-0.007(1)	-0.008(1)	0.013(1)
O2	0.026(1)	0.047(1)	0.049(1)	-0.030(1)	-0.005(1)	0.022(1)
O3	0.016(1)	0.010(1)	0.026(1)	-0.001(1)	0(1)	0.008(1)
O4	0.023(1)	0.039(1)	0.034(1)	0.013(1)	-0.012(1)	0.013(1)

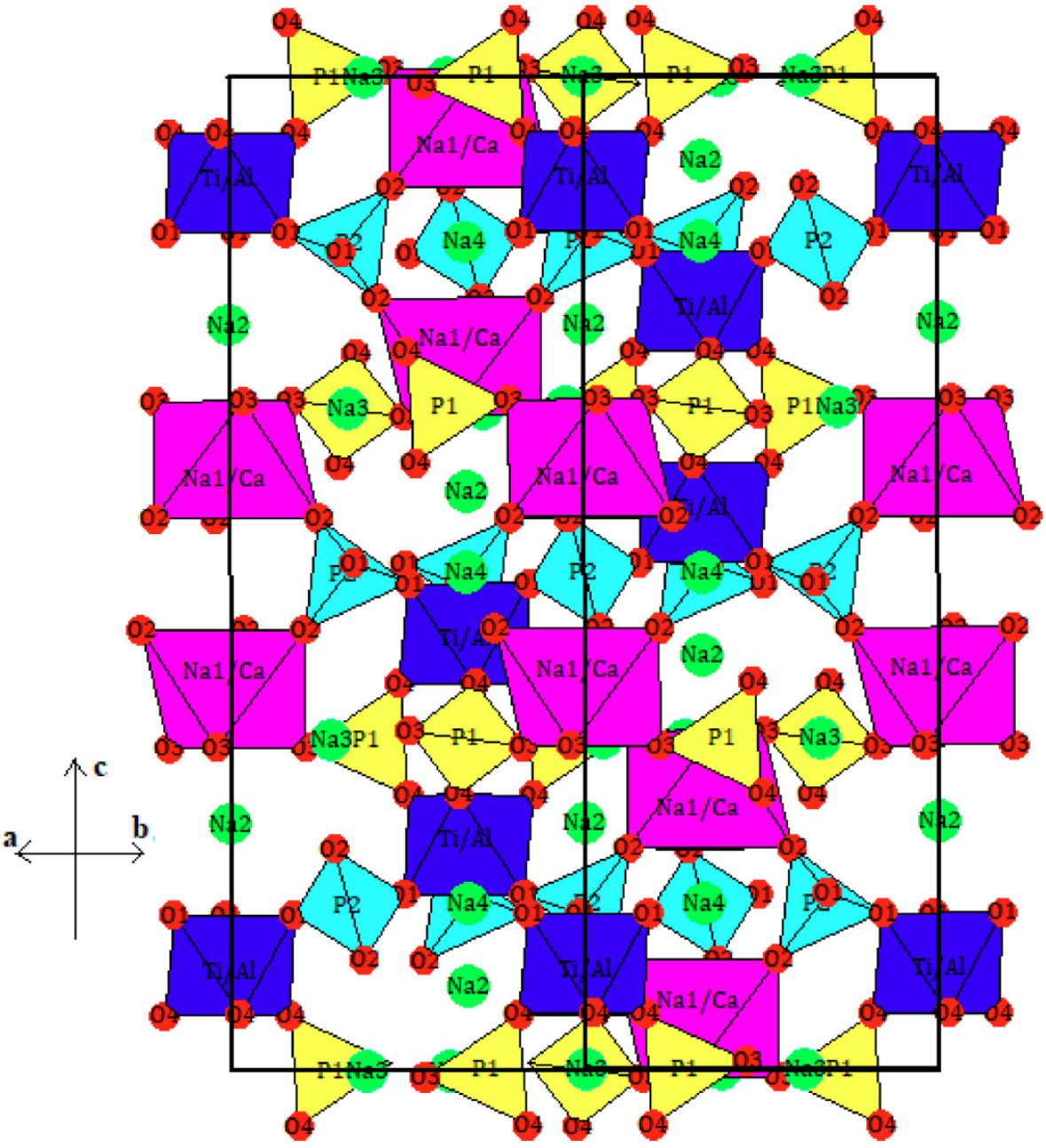

Fig. 5. Structure of $Na_{3.89}Ca_{0.67}Al_{0.23}Ti_{0.77}(PO_4)_3$ along the c axis.

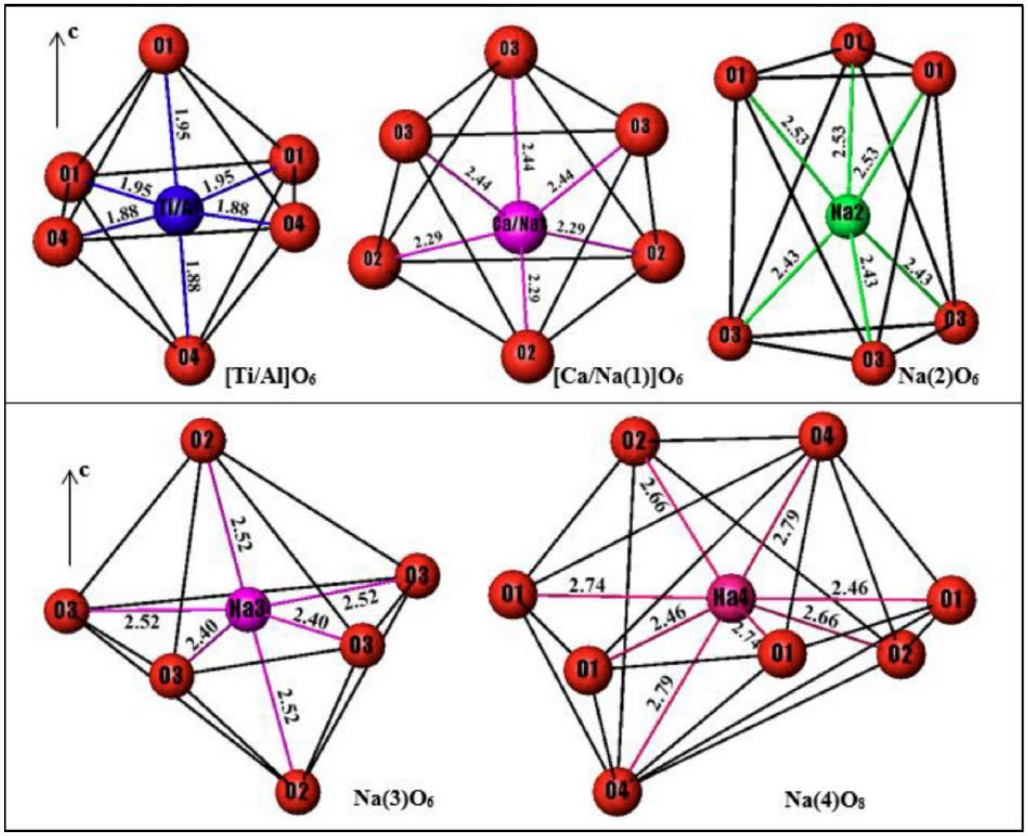

Fig. 6. Environments in A [(Al/TiO_6), ($Na1/CaO_6$)], M (1) [$Na2O_6$] and M (2) [$Na3O_6$, $Na4O_8$] sites in $Na_{3.89}Ca_{0.67}Al_{0.23}Ti_{0.77}(PO_4)_3$ and Metal-Oxygen distances (Å).

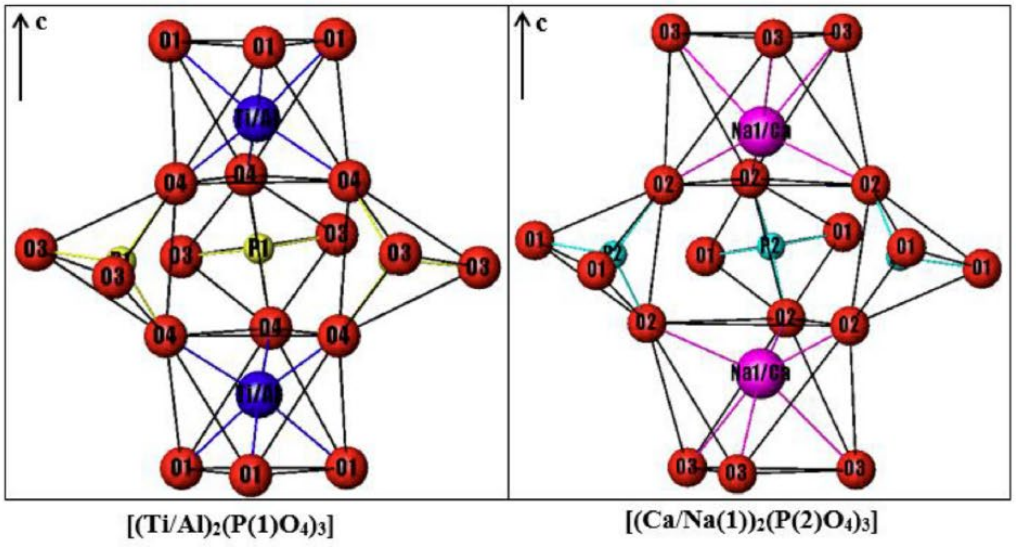

Fig. 7. [$(Al/Ti)_2(P1O_4)_3$] and [$(Na1/Ca)_2(P2O_4)_3$] motifs in $Na_{3.89}Ca_{0.67}Al_{0.23}Ti_{0.77}(PO_4)_3$.

and Na4 (expected 1), 5.03 and 5.06 for P1 and P2 (expected 5). The difference observed between the calculated and expected values for ions in A (Na1/Ca and Al/Ti) and M(2) (Na4) sites, is probably due to the distortion of these polyhedra. For the other ions, the obtained values are very close to the expected ones. The substitution in $Na_3CaTi(PO_4)_3$ (a_h = 8.985 Å; c_h = 21.920 Å) of Al^{3+} for Ti^{4+} ($[Na]_{M1}[Na_{2+x\ +\ y}]_{M2}[Na_xCa_{1-x}Al_yTi_{1-y}]_A(PO_4)_3$ with x = 0.33 and y = 0.23; a_h = 8.998 Å; c_h=21.813 Å) induces a decrease of the c parameter value, due to the decrease of the size of the cation located at the octahedral A site (r_{Al3+}= 0.53 Å; r_{Ti4+}= 0.61 Å) and to the decrease of the strength of the $Na^+(M1)$ – A^{n+} electrostatic repulsions [$Na^+(M1)$ – $Na^+{}_xCa^{2+}{}_{1-x}$

Table 6
Powder X-ray diffraction data of $Na_{3.89}Ca_{0.67}Al_{0.23}Ti_{0.77}(PO_4)_3$.

h k l	d_{obs} (Å)	d_{cal} (Å)	I/I_0*100
1 0 1	7.308	7.333	21
0 0 3		7.270	
0 1 2	6.317	6.337	9
1 0 4	4.458	4.466	28
1 1 3	3.817	3.823	91
0 0 6	3.629	3.635	23
0 2 4	3.163	3.168	14
2 1 1	2.912	2.916	30
2 0 5		2.904	
1 1 6	2.822	2.827	100
3 0 0	2.591	2.595	61
2 1 4		2.590	
3 0 3	2.439	2.444	6
1 2 5		2.440	
0 2 7		2.433	
2 2 0	2.245	2.248	4
2 0 8	2.230	2.233	5
1 3 1	2.145	2.149	16
2 2 3		2.147	
3 1 2	2.115	2.118	4
3 0 6		2.112	
1 3 4	1.998	2.008	8
1 2 8		2.000	
3 1 5	1.933	1.935	4
2 2 6	1.909	1.912	29
0 2 10		1.903	
0 0 12	1.815	1.817	6
0 4 5	1.773	1.778	7
1 3 7		1.775	
3 0 6		1.771	
2 1 10	1.750	1.752	9
3 2 4	1.695	1.697	8
3 1 8		1.693	
4 1 3	1.651	1.654	3
2 3 5		1.653	
4 0 7		1.651	
4 1 6	1.537	1.539	11
1 3 10		1.535	
3 3 0	1.498	1.498	6
0 3 12	1.489	1.489	6
2 4 1	1.468	1.468	3
1 5 2	1.385	1.387	4
3 3 6		1.385	
1 1 15		1.383	
5 1 4	1.353	1.355	3
5 0 8		1.352	

(A) < Na^+(M1) – Ca^{2+} (A) and Na^+(M1) – $Al^{3+}{}_yTi^{4+}{}_{1-y(A)}$ < Na^+(M1) – Ti^{4+}(A); $x = 0.33$ and $y = 0.23$]. The main average atomic distances and angles obtained from PXRD Rietveld refinement of $Na_{3.89}Ca_{0.67}Al_{0.23}Ti_{0.77}(PO_4)_3$ are close to those obtained from the SCXRD structure determination of this phosphate (Table 4).

3.4. Vibrational study of $Na_{3.89}Ca_{0.67}Al_{0.23}Ti_{0.77}(PO_4)_3$

3.4.1. Crystalline compound

Vibrational analysis for an isolated $PO_4{}^{3-}$ anion with point group Td leads to four modes: A1[(υ_1: $\upsilon_s(PO_4)$], E[(υ_2: $\delta_s(PO_4)$] and $2T_2$[υ_3: $\upsilon_{as}(PO_4)$ *and* υ_4: $\delta_{as}(PO_4)$]. All of them are Raman-active modes whereas only υ_3 and υ_4 are infrared-active modes. In $Na_{3.89}Ca_{0.67}Al_{0.23}Ti_{0.77}(PO_4)_3$ phosphate, Nasicon structural type (R32 space group), the P atom is in a C_2 symmetry site. Therefore, for the stretching vibrations we can expect 12 Raman-active modes: [$(2A_1 + 2E)(\upsilon_1) + (2A_1 + 6E)(\upsilon_3)$] and 12 IR-active modes: [$2E(\upsilon_1) + (4A_2 + 6E)(\upsilon_3)$]. For the bending vibrations we achieved 16 Raman-active modes: [$(4A_1 + 4E)(\upsilon_2) + (2A_1 + 6E)(\upsilon_4)$] and 14 IR-active modes: [$(4E)(\upsilon_2) + (4A_2 + 6E)\ (\upsilon_4)$] [49,50].

The Raman and infrared spectra of crystalline $Na_{3.89}Ca_{0.67}Al_{0.23}Ti_{0.77}(PO_4)_3$ (Fig. 8) are dominated by the vibrations of PO_4 tetrahedra. The observed peaks are very broad due to the disorder, around PO_4 tetrahedra, in A (Na/Ca; Al/Ti) and M(2) (Na/vacancy) sites. The high frequency part (800 – 1300 cm^{-1}) corresponds to the stretching vibration of $\upsilon_{as}(PO_4)$ and $\upsilon_s(PO_4)$ tetrahedra ($\upsilon_{as} > \upsilon_s$). The peak around 1039 cm^{-1} can be attributed to the vibrations of the diphosphate $Na_4P_2O_7$ present as impurity in the sample [51]. The broad shoulder observed around 763 cm^{-1} (731cm^{-1} in IR) can be attributed to the vibrations of Ti-O and P-O-P bonds of TiO_2 and $Na_4P_2O_7$ impurities [51–54]. Indeed, for all Nasicon-type phosphates, in which tetrahedra, as well as octahedra, are isolated from each other, no peak is observed in 700–800 cm^{-1} region [28,50,55,56]. The peaks observed between 700 and 400 cm^{-1} are assigned to the angular deformation modes $\delta_s(PO_4)$ and $\delta_{as}(PO_4)$ and to the vibrations of Ti-O and Al-O bonds in TiO_6 and AlO_6 octahedra [28,50,55,57,58]. The peaks below 400 cm^{-1} are attributed to the external modes and to the lattice vibrations: $PO_4{}^{3-}$ rotations and translations of Na^+, Ca^{2+}, Al^{3+}, Ti^{4+} and $PO_4{}^{3-}$ ions. The Raman and IR band positions of PO_4 modes, observed in the present NaCaAlTi-phosphate, are close to those obtained for other Nasicon-type phosphates [28,50,55,56].

3.4.2. Vitreous compound

The peaks observed in the high frequency region 800 – 1250 cm^{-1} are due to monophosphate and diphosphate groups. The peak in Raman spectrum at ~1035 cm^{-1}, relatively sharp, is due to $P_2O_7{}^{4-}$ diphosphate ions [52,54,59,60]. The strong Raman peak, between 700 and 800 cm^{-1}, observed also in titanium oxyphosphates and in titanium phosphate glasses, is assigned to Ti-O vibrations in the -Ti-O-Ti-O- chains [42,43,61-63]. It indicates that the glass structure contains TiO_6 octahedra which are linked by corners and form short -Ti-O-Ti-O- chains. These chains are certainly linked to phosphate groups to form -Ti-O-P- linkages. The peaks observed between 400 and 700 cm^{-1} are attributed to O-P-O and P-O-P deformations (δ_2 and δ_4 PO_4 modes) and to Ti-O and Al-O vibrations of TiO_6 [64] and AlO_6 octahedra [65]. The peaks observed below 400 cm^{-1} are attributed to the external modes and to the lattice vibrations.

3.5. UV–Visible study of $Na_{3.89}Ca_{0.67}Al_{0.23}Ti_{0.77}(PO_4)_3$

Fig. 9 shows the powder diffuse reflectance spectra of crystalline and vitreous $Na_{3.89}Ca_{0.67}Al_{0.23}Ti_{0.77}(PO_4)_3$ and TiO_2 rutile. Crystalline $Na_{3.89}Ca_{0.67}Al_{0.23}Ti_{0.77}(PO_4)_3$ presents three bands labeled A (λ = 350 nm), B (λ = 275 nm) and C (λ = 225 nm). The spectrum of the vitreous compound shows an intense and wide band covering the B and C absorption bands. The absorption bands observed in TiO_2 is ascribed to the O-Ti electronic charge transfer, according to the following mechanism:

$$O^{2-}\left(2p^6\right) + Ti^{4+}\left(3d^0\right) \rightarrow O^{-}\left(2p^5\right) + Ti^{3+}\left(3d^1\right)$$

The B band is similar to that observed in Nasicon-type titanium phosphates [42]. The values of the O-Ti charge transfer gap energy (Eg) of these crystalline phosphates (Eg ~ 3.54 eV) is larger than that of TiO_2 (Eg = 3.00 eV). In TiO_2 every oxygen ion O^{2-} is linked to two Ti^{4+} ions (Ti-O-Ti), while in Nasicon-type titanium phosphates every O^{2-} is linked to Ti^{4+} and P^{5+} (Ti-O-P) (Fig. 10). As P-O bond is more covalent than Ti-O bond, the transfer of an electron from O^{2-} to Ti^{4+} is more difficult in crystalline $Na_{3.89}Ca_{0.67}Al_{0.23}Ti_{0.77}(PO_4)_3$ than in TiO_2 and explains the high value of Eg obtained for the phosphates. The C band observed at high energy (E = 5.39 eV) is attributed to O-Al charge transfer as reported for aluminum phosphate (E = 5.41 eV) [66]:

$$O^{2-}\left(2p^6\right) + Al^{3+}\left(3s^0\right) \rightarrow O^{-}\left(2p^5\right) + Al^{2+}\left(3s^1\right)$$

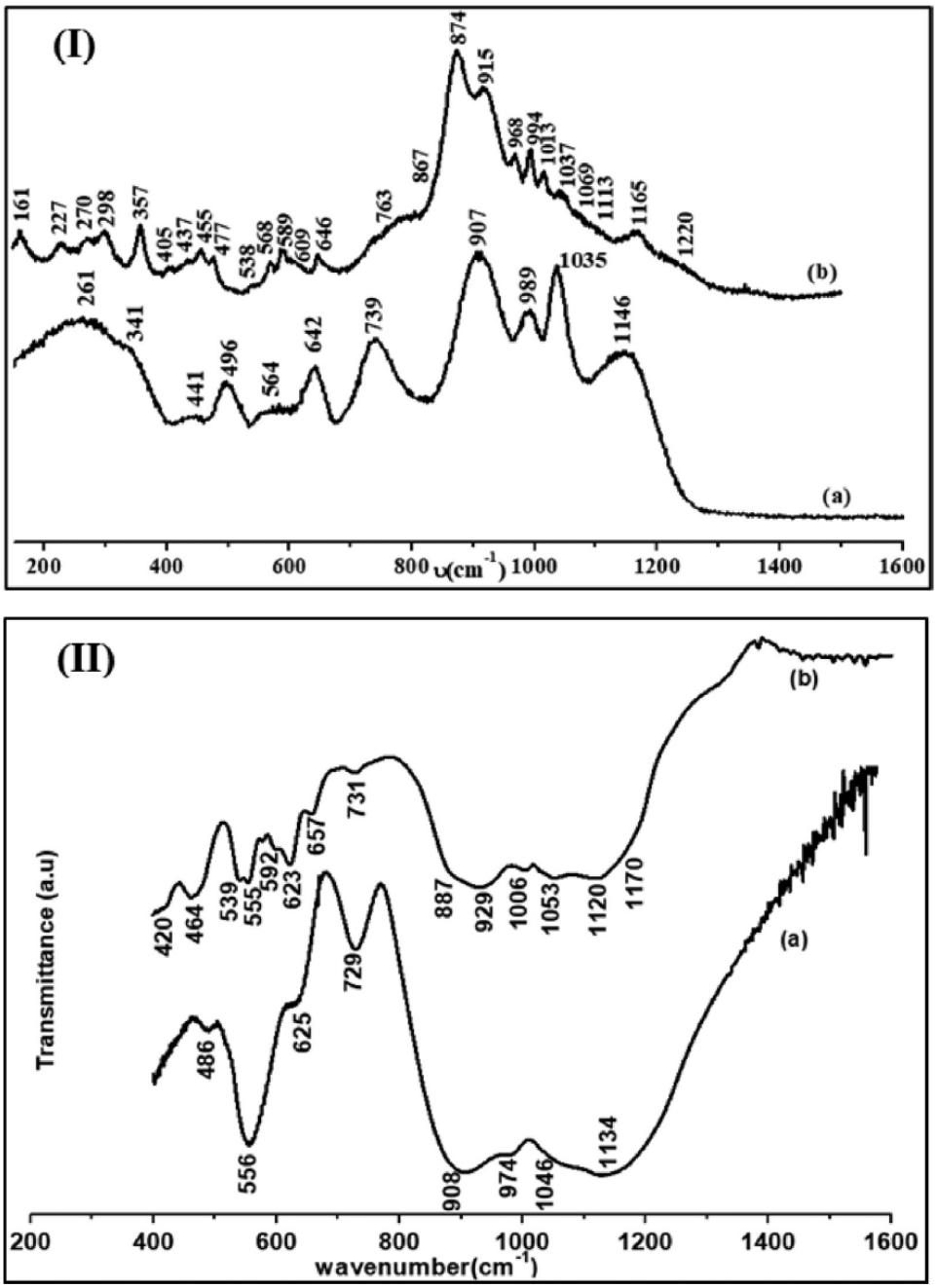

Fig. 8. Raman (I) and infrared (II) spectra of (a) vitreous and (b) crystalline forms of $Na_{3.89}Ca_{0.67}Al_{0.23}Ti_{0.77}(PO_4)_3$.

The A band is similar to that observed in TiO_2 but with less intensity. This band is absent in the glassy compound. The powder X-ray diffraction of crystalline $Na_{3.89}Ca_{0.67}Al_{0.23}Ti_{0.77}(PO_4)_3$ sample showed the presence of TiO_2 as impurity (Fig. 2). So, we attribute A band to the O-Ti charge transfer in TiO_2. Indeed, previous studies of Ti^{4+}- doped compounds [crystalline $K_2Zr_{1-x}Ti_xSi_3O_9$ ($0 \leq x \leq 0.02$) [67] and $20Na_2O$-10CaO-(1-x)SiO_2-xTiO_2 ($x = 0.01$) glass [68]] showed that UV-visible spectroscopy is very sensible to low amount of Ti^{4+} ions. Diffuse reflectance spectra of these compounds showed absorption near 300 nm attributed to O-Ti charge transfer. For the glassy $Na_{3.89}Ca_{0.67}Al_{0.23}Ti_{0.77}(PO_4)_3$, the value of the gap (Eg = 3.33 eV) is intermediate between those of TiO_2 (3.00 eV) and Nasicon titanium phosphates (~ 3.54 eV) and very close to that obtained for titanium oxyphosphates (3.37 eV) [69]. This evolution can be explained by the structure of these compounds. In TiO_2 every TiO_6 octahedron is surrounded by six other TiO_6 octahedra, in titanium oxyphosphates every TiO_6 octahedron is surrounded by two TiO_6 octahedra and four PO_4 tetrahedra, while in Nasicon phosphates every TiO_6 octahedron is surrounded by six PO_4 tetrahedra (Fig. 10). As P-O bond is more covalent than Ti-O bond, the value of the gap increases when we replace TiO_6 octahedra by PO_4 tetrahedra.

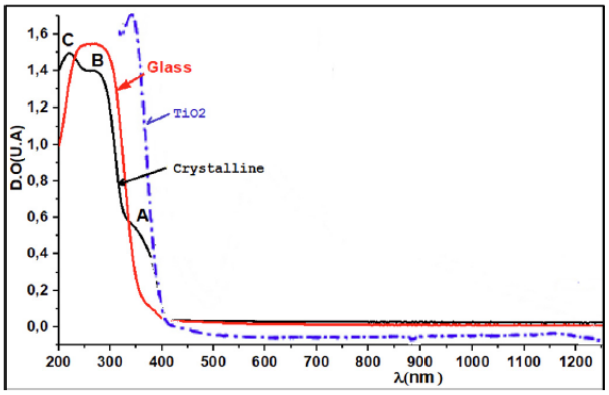

Fig. 9. Diffuse reflectance spectra of crystalline and vitreous forms of $Na_{3.89}Ca_{0.67}Al_{0.23}Ti_{0.77}(PO_4)_3$ and of TiO_2 (rutile).

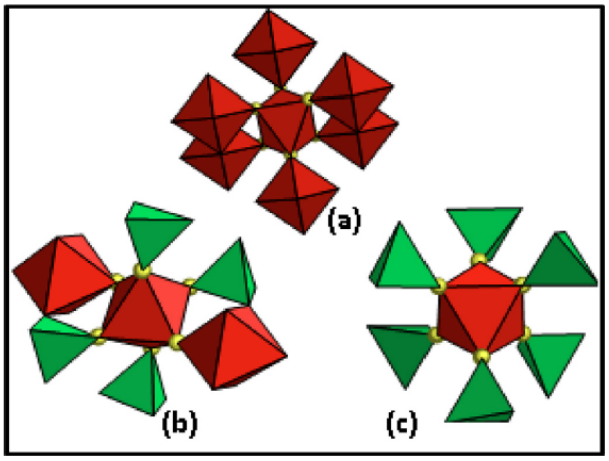

Fig. 10. Environment around TiO_6 octahedron in (a) TiO_2 rutile, (b) titanium oxyphosphates and in (c) Nasicon-type phosphates.

4. Conclusion

A new crystalline and vitreous phosphate composition $Na_{3.89}Ca_{0.67}Al_{0.23}Ti_{0.77}(PO_4)_3$ has been synthesized and structurally characterized. The structure of the crystalline compound, determined from single crystal and microcrystalline powder, consists of a 3D network of PO_4 tetrahedra and AO_6 (A= Na/Ca; Al/Ti) octahedra sharing corners. One of the two positions of A sites is statistically occupied by Na^+ and Ca^{2+}, the other position is statistically occupied by Al^{3+} and Ti^{4+}. The remaining sodium atoms occupy totally the M(1) site and partially the M(2) sites. Raman and IR study is consistent with the crystal structure. The structure of the glass contains PO_4 and P_2O_7 groups and short – Ti – O – Ti – O – chains. Reflectance diffusion spectra showed bands attributed to O-Ti and O-Al electronic charge transfers.

Credit authorship contribution statement

Ahmed Nazih: Conceptualization, methodology, visualization, validation, writing - original draft, formal analysis, review and editing.

Stanislas Péchev : single crystal structure, discussion and Validation

Matias Velazquez : discussion and Validation

Michel Couzi : Raman measurements

Abdelaziz El Jazouli : Conceptualization, methodology, visualization, validation, writing - original draft, formal analysis, review and editing

Saida Krimi: Conceptualization, methodology, visualization, validation, writing - original draft, formal analysis, review –editing and supervision.

Declaration of Competing Interest

The authors declare that they have no known competing financial interests or personal relationships that could have appeared to influence the work reported in this paper.

Data availability

No data was used for the research described in the article.

Acknowledgements

The authors thank CNRST/Morocco - CNRS/France (Agreement No. 24494) and the Volubilis Committee (Integrated Action No. MA/10/229) for their financial support. They thank also Pr. H. Oudadesse from University of Rennes 1 - France, for the ICP analysis.

Supplementary materials

Supplementary material associated with this article can be found, in the online version, at doi:10.1016/j.molstruc.2023.135129.

References

[1] J.B. Goodenough, H.Y–P. Hong, A. Kafalas, Fast Na^+-ion transport in skeleton structures, Mat. Res. Bull. 11 (1976) 203–220, doi:10.1016/0025-5408(76)90077-5.

[2] H. Rusdi, N.S. Mohamed, R.H.Y. Subban, R. Rusdi, Enhancement of electrical properties for Nasicon-type solid electrolytes ($LiSn_2P_3O_{12}$) via aluminium substitution, J. Sci. Adv. Mater. Devices 5 (2020) 368–377, doi:10.1016/j.jsamd.2020.06.003.

[3] Y. Fang, J. Zhang, L. Xiao, X. Ai, Y. Cao, H. Yang, Phosphate framework electrode materials for sodium ion batteries, Adv. Sci. 4 (5) (2017) 1600392, doi:10.1002/advs.201600392.

[4] K. Waetzig, A. Rost, C. Heubner, M. Coeler, K. Nikolowski, M. Wolter, J. Schilm, Synthesis and sintering of $Li_{1.3}Al_{0.3}Ti_{1.7}(PO_4)_3$ (LATP) electrolyte for ceramics with improved Li^+ conductivity, J. Alloys Compounds. 818 (2019) 153237, doi:10.1016/j.jallcom.2019.153237.

[5] C. Delmas, A. Nadiri; J.L. Souberyoux, The Nasicon-type titanium phosphates ATi2(PO4)3, Solid State Ionics. 28-30 (1988) 419–423. doi:10.1016/S0167-2738(88)80075-4.

[6] C. Masquelier, L. Croguennec, Polyanionic (phosphates, silicates, sulphates) frameworks as electrode materials for rechargeable Li (or Na) batteries, Chem. Rev. 113 (2013) 6552, doi:10.1021/cr3001862.

[7] R. Rustum, D.K. Agrawal, J. Alamo, R.A. Roy, [CTP]: a new structural family of near-zero expansion ceramics, Mat. Res. Bull. 19 (4) (1984) 471–477, doi:10.1016/0025-5408(84)90108-9.

[8] J.M. Heintz, L. Rabardel, M. Al Qaraoui, M. Alami Talbi, R. Brochu, G. Le Flem, New low thermal expansion ceramics: sintering and thermal behaviour of $Ln_{1/3}Zr_2(PO_4)_3$ – based composites, J. Alloys Compounds. 250 (1997) 515–519, doi:10.1016/S0925-8388(96)02631-X.

[9] M. Attari, P. Fabry, H. Mallié, G. Quezel, A new double-jet cell for fast ion-sensitive electrodes, Sens. Actuators B 15 (1–3) (1993) 173–178, doi:10.1016/0925-4005(93)85045-C.

[10] A. Mbandza, E. Bordes, P. Courtine, A. El Jazouli, J.L. Soubeyroux, G.Le Flem, P. Hagenmuller, The Nasicon-type copper(I) titanium phosphate $CuTi_2(PO_4)_3$: structure and chemical properties, React. Solids. 5 (4) (1988) 315–321, doi:10.1016/0168-7336(88)80030-5.

[11] A. Serghini, M. Kacimi, M. Ziyad, R. Brochu, Décomposition du butanol-2 sur les phosphates de cuivre et de zirconium de type structural Nasicon, J. Chem. Phys. 85 (1988) 499–504, doi:10.1051/jcp/1988850499.

[12] Y. He, B. Quan, Y. Wang, C. Cheng, B. Wang, Photoluminescence characteristics of Nasicon materials, Mater. Lett. 61 (2007) 4519–4521, doi:10.1016/j.matlet.2007.02.072.

[13] A. Mouline, M. Alami, R. Brochu, R. Olazcuaga, C. Parent, G.Le Flem, The structure and luminescent properties of $Mn_{0.5}Zr_2(PO_4)_3$, Mat, Res. Bull. 35 (2000) 899–908, doi:10.1016/S0025-5408(00)00277-4.

[14] N. Anantharamulu, K. Koteswara Rao, G. Rambabu, B. Vijaya Kumar, V. Radha, M. Vithal, A wide-ranging review on Nasicon type materials, J. Med. Aromat. Plant Sci. 46 (2011) 2821–2837, doi:10.1007/s10853-011-5302-5.

[15] L.O. Hagman, P. Kierkegaad, The crystal structure of $NaMe_2^{IV}(PO_4)_3$ (Me = Ge, Ti, Zr), Acta Chem. Scand. 22 (1968) 1822–1832, doi:10.3891/acta.chem.scand.22-1822.

[16] G.V. Subba Rao, U.V. Varadaraju, K.A. Thomas, B. Sivasankar, Metal atom incorporation studies on the phases with NZP structure: $NbTiP_3O_{12}$, J. Solid State Chem. 70 (1987) 101–107, doi:10.1016/0022-4596(87)90183-6.

[17] D. Zhao, P. Liang, L. Su, H. Chang, S. Yan, $Al_{0.5}Nb_{1.5}(PO_4)_3$, Acta Crystallogr. E67 (2011) i23, doi:10.1107/S1600536811003886.

[18] A. El Jazouli, A. El Bouari, H. Fakrane, A. Housni, M. Lamire, I. Mansouri, R. Olazcuaga, G. Le Flem, Crystallochemistry and structural study of some Nasicon-like phosphates, J. Alloys Compd. 262-263 (1997) 49–53, doi:10.1016/s0925-8388(97)00466-0.

[19] O. Mentre, F. Abraham, B. Deffontaines, P. Vast, Structural study and conductivity properties of $Ca_{1-x}Na_{2x}Ti_4(PO_4)_6$ solid solution, Solid State Ionic 72 (1994) 293–299, doi:10.1016/0167-2738(94)90162-7.

[20] H. Fakrane, A. Aatiq, M. Lamire, A. El Jazouli, C. Delmas, Chemical, structural and magnetic studies of $Mn_{0.5}Ti_2(PO_4)_3$ and its solid solution with $NaTi_2(PO_4)_3$, Ann. Chim. Sci. Mat. 23 (1–2) (1998) 81–84, doi:10.1016/S0151-9107(98)80028-7.

[21] S. Benmokhtar, A. El Jazouli, A. Aatiq, J.P. Chaminade, P. Gravereau, A. Wattiaux, L. Fournes, J.C. Grenier, Synthesis, structure and characterisation of $Fe_{0.5}Ti_2(PO_4)_3$: a new material with Nasicon-like structure, J. Solid State Chem. 180 (2007) 2004–2012, doi:10.1016/j.jssc.2007.04.014.

[22] S. Benmokhtar, A. El Jazouli, J.P. Chaminade, P. Gravereau, A. Wattiaux, L. Fournès, J.C. Grenier, Elaboration and characterisation of two new iron titanium phosphates $Fe_{0.5}TiO(PO_4)$ and $Fe_{0.5}Ti_2(PO_4)_3$, Phosphorus Res. Bull. 15 (2004) 140–142, doi:10.3363/prb1992.15.0_140.

[23] A. El Bouari, A. El Jazouli, J.M. Dance, G. Le Flem, R. Olazcuaga, A new Nasicon-like phosphate $Co_{0.5}Ti_2(PO_4)_3$, Adv. Mat. Res. 1-2 (1994) 173–176, doi:10.4028/www.scientific.net/AMR.1-2.173.

[24] R. Olazcuaga, J.M. Dance, G. Le Flem, J. Derouet, L. Beaury, P. Porcher, A. El Bouari, A. El Jazouli, A new Nasicon-type phosphate $Co_{0.5}Ti_2(PO_4)_3$: I. Elaboration, optical and magnetic properties, J. Solid State Chem. 143 (1999) 224–229, doi:10.1006/jssc.1998.8097.

[25] A. El Bouari, A. El Jazouli, Crystal structure of $Pb_{0.5}Ti_2(PO_4)_3$, Phosphorus Res. Bull. 15 (2004) 136–139, doi:10.3363/prb1992.15.0_136.

[26] A. Housni, I. Mansouri, A. El Jazouli, R. Olazcuaga L. Fournes, G. Le Flem, Crystal structure, magnetic and mössbauer investigation of a new Nasicon-type phosphate $Ba_{0.5}FeNb(PO_4)_3$, Ann. Chim. Sc. Mat. 23 (1–2) (1998) 73–76, doi:10.1016/S0151-9107(98)80026-3.

[27] A. Aatiq, M. Menetrier, L. Croguennec, E. Suard, C. Delmas, On the structure of $Li_3Ti_2(PO_4)_3$, J. Mater. Chem. 12 (2002) 2971–2978, doi:10.1039/b203652p.

[28] M. Chakir, A. El Jazouli, D. de Waal, Synthesis, crystal structure and spectroscopy properties of $Na_3AZr(PO_4)_3$ (A = Mg, Ni) and $Li_{2.6}Na_{0.4}NiZr(PO_4)_3$ phosphates, J. Solid State Chem. 179 (2006) 1883–1891, doi:10.1016/j.jssc.2006.03.003.

[29] M. Chakir, A. El Jazouli, J.P. Chaminade, Synthesis and crystal structure of $Na_{3.5}Cr_{1.5}Co_{0.5}(PO_4)_3$ phosphate, Powder Diffr. 21 (3) (2006) 210–213, doi:10.1154/1.2190689.

[30] E.A. Asabina, V.I. Pet'kov, E.R. Gobechiya, Y.K. Kabalov, K.V. Pokholok, V.S. Kurazhkovskaya, Synthesis and crystal structure of phosphates $A_2FeTi(PO_4)_3$ (A = Na, Rb), Russ. J. Inorg. Chem. 53 (1) (2008) 40–47, doi:10.1134/s0036023608010075.

[31] A. El Bouari, A. El Jazouli, S. Benmokhtar, P. Gravereau, A. Wattiaux, Synthesis, structure, magnetic, optical and Mössbauer properties of $Na_2FeSn(PO_4)_3$, J. Alloys Compd. 503 (2010) 480–484, doi:10.1016/j.jallcom.2010.05.037.

[32] S. Krimi, I. Mansouri, A. El Jazouli, J.P. Chaminade, P. Gravereau, G. Le Flem, The structure of $Na_5Ti(PO_4)_3$, J. Solid State Chem. 105 (1993) 561–566, doi:10.1006/jssc.1993.1248.

[33] J.P. Boilot, G. Collin, R. Comes, Zirconium deficiency in Nasicon-type compounds: crystal structure of $Na_5Zr(PO_4)_3$, J. Solid State Chem. 50 (1983) 91–99, doi:10.1016/0022-4596(83)90236-0.

[34] C. Delmas, F. Cherkaoui, P. Hagenmuller, Ionic conductivity in a new Nasicon related solid solution: $Na_{3+y}Cr_{2-y}Mg_y(PO_4)_3$. An optical characterization of the skeleton covalency, Mater. Res. Bull. 21 (1986) 469–477, doi:10.1016/0025-5408(86)90013-9.

[35] B. Manoun, A. El Jazouli, S. Krimi, A. Lachgar, Synthesis and crystallochemistry of $Na_4CrNi(PO_4)_3$, Powder Diffraction. 19 (2) (2004) 162–164, doi:10.1154/1.1596632.

[36] I.V. Zatovsky, N. Yu. Strutynska, I.V. Ogorodnyk, V.N. Baumer, N.S. Slobodyanik, M.M. Yatskin, I.V. Odynets, Peculiarity of formation of the Nasicon-related phosphates in the space group R32: synthesis and crystal structures of $Na_4M^{II}Al(PO_4)_3$ (M^{II} = Mg, Mn), Struct. Chem. 27 (1) (2015) 323–330, doi:10.1007/s11224-015-0713-6.

[37] M.J. Aragon, C. Vidal-Abarca, P. Lavela, J.L. Tirado, High reversible sodium insertion into iron substituted $Na_{1+x}Ti_{2-x}Fe_x(PO_4)_3$, J. Power Sources 252 (2014) 208–213, doi:10.1016/j.jpowsour.2013.12.006.

[38] Y. Hasegawa, N. Imanaka, Effect of the lattice volume on the Al^{3+} ion conduction in Nasicon type solid electrolyte, Solid State Ionic. 176 (2005) 2499–2503, doi:10.1016/j.ssi.2005.02.028.

[39] P. Maldonado-Manso, M.C. Martin-Sedeno, S. Bruque, J. Sanz, E.R. Losilla, Unexpected cationic distribution in tetrahedral/octahedral sites in nominal $Li_{1+x}Al_xGe_{2-x}(PO_4)_3$ Nasicon series, Solid State Ionic. 178 (2007) 43–52, doi:10.1016/j.ssi.2006.11.016.

[40] N. Imanishi, M. Matsui, Y. Takeda, O. Yamamoto, Lithium ion conducting solid electrolytes for aqueous lithium-air batteries, Electrochemistry 82 (11) (2014) 938–945, doi:10.5796/electrochemistry.82.938.

[41] S. Krimi, I. Mansouri, A. El Jazouli, J.P. Chaminade, P. Gravereau, G.Le Flem, Investigation of the glass-crystal transition of $Na_5Ti(PO_4)_3$, J. Alloys Compd. 188 (1992) 120–122, doi:10.1016/0925-8388(92)90657-U.

[42] S. Krimi, A. El Jazouli, A. Lachgar, L. Rabardel, D. de Waal, J.R. Ramos-Barrado, Glass – crystal transformation of $Na_{5-2x}Ca_xTi(PO_4)_3$ phosphates, Ann. Chim. Sc. Mater. 25 (2000) S75–S78.

[43] S. Lamrhari, Z. El Khalidi, S. Krimi, M. Haddad, M. Couzi, A. Lachgar, A. El Jazouli, Synthesis and structural characterization of phosphate-based Nasiglasses $Na_3Ca_{1-x}Mn_xTi(PO_4)_3$ ($0 \le x \le 1$), J. Mater. Environ. Sci. 9 (11) (2018) 3009–3018 http://www.jmaterenvironsci.com.

[44] G.M. Sheldrick, Crystal structure refinement with SHELXL, Acta Cryst. C 71 (2015) 3–8, doi:10.1107/S2053229614024218.

[45] I.D. Brown, D. Altermatt, Bond-valence parameters obtained from a systematic analysis of the Inorganic Crystal Structure Database, Acta Cryst. B 41 (1985) 244–247, doi:10.1107/S0108768185002063.

[46] H.M. Rietveld, Line profiles of neutron powder-diffraction peaks for structure refinement, Acta Cryst. 22 (1967) 151–152, doi:10.1107/S0365110×67000234.

[47] J. Rodriguez-Carvajal, Fullprof: a program for Rietveld refinement and pattern matching analysis, in: Abstract of the Satellite Meeting on Powder Diffraction of the XV Congress of the IUCr, 1990, p. 127. Toulouse, France.

[48] R.D. Shannon, C.T. Prewitt, Effective Ionic Radii in Oxides and Fluorides, Acta Cryst., B 25 (1969) 925–946, doi:10.1107/S0567740869003220.

[49] F.A. Cotton, in: Chemical Applications of Group Theory, 249, 3rd ed, Wiley, Interscience, NY, 1990, p. 394, doi:10.1016/0022-2860(91)85088-K.

[50] P. Tarte, A. Rulmont, C. Merckaert-Ansay, Vibrational spectrum of Nasicon-like, rhombohedral orthophosphates $M^IM^{IV}_2(PO_4)_3$, Spectrochim. Acta A Mol. Biomol. Spectrosc. 42 (9) (1986) 1009–1016, doi:10.1016/0584-8539(86)80012-5.

[51] L. Popovic, D. de Waal, J.C.A. Boeyens, Correlation between Raman wavenumbers and P-O bond lengths in crystalline inorganic phosphates, J. Raman Spectrosc. 36 (2005) 2–11, doi:10.1002/jrs.1253.

[52] C. Bhongale, A. Ghule, R. Murugan, H. Chang, Thermo-Raman studies on dehydration of $Na_4P_2O_7{,}10H_2O$ and phase transformations of $Na_4P_2O_7$, J. Therm. Anal. Cal. 65 (2001) 891–905, doi:10.1023/a:1011996620063.

[53] U. Balachandran. N. G. Eror, Raman spectra of titanium dioxide, J. Solid State Chem. 42 (1982) 276–282, doi:10.1016/0022-4596(82)90006-8.

[54] S. Kaoua, S. Krimi, S. Péchev, P. Gravereau, J.-.P. Chaminade, M. Couzi, A. El Jazouli, Synthesis, crystal structure, and vibrational spectroscopic and UV–visible studies of $Cs_2MnP_2O_7$, J. Solid State Chem. 198 (2013) 379–385, doi:10.1016/j.jssc.2012.10.016.

[55] A. El Jazouli, S. Krimi, B. Manoun, J.P. Chaminade, P. Gravereau, D. de Waal, Preparation and structural characterization of two new titanium phosphates $Na_4Ca_{0.5}Ti(PO_4)_3$ and $Ni_{0.5}TiOPO_4$, Ann. Chim. Sci. Mat. 23 (1998) 7–10, doi:10.1016/S0151-9107(98)80001-9.

[56] R. Pikl, D. de Waal, A. Aatiq, A. El Jazouli, Vibrational spectra and factor group analysis of $Mn_{(0.5+x)}Ti_{(2-2x)}Cr_{2x}(PO_4)_3$ {$0 \le x \le 0.50$}, Vibr. Spectrosc. 16 (1998) 137–143, doi:10.1016/S0924-2031(98)00007-1.

[57] A. John, D. Philip, K.R. Morgan, S. Devanarayanan, IR and Raman spectra of two layered aluminium phosphates $Co(en)_3Al_3P_4O_{16}{\cdot}3H_2O$ and $[NH_4]_3[Co(NH_3)_6]_3[Al_2(PO_4)_4]_2{\cdot}2H_2O$, Spectrochimica Acta Part A 56 (2000) 2715–2723, doi:10.1016/S1386-1425(00)00314-0.

[58] J. Thapa, B. Liu, S.D. Woodruff, B.T. Chorpening, M.P. Buric, Raman scattering in single-crystal sapphire at elevated temperatures, Appl. Opt. 56 (31) (2017) 8598–8606, doi:10.1364/ao.56.008598.

[59] M. Harcharras, A. Ennaciri, A. Rulmont, B. Gilbert, Vibrational spectra and structures of double diphosphates $M_2CdP_2O_7$ (M = Li, Na, K, Rb, Cs), Spectrochimca. Acta A 53 (1997) 345–352, doi:10.1016/S1386-1425(96)01782-9.

[60] S. Krimi, A. El Jazouli, L. Rabardel, M. Couzi, I. Mansouri, G. Le Flem, Glass formation in the Na_2O-TiO_2-P_2O_5, J. Solid State Chem. 102 (1993) 400–407, doi:10.1006/jssc.1993.1051.

[61] C.E. Bamberger, G.M. Begun, O.B. Cavin, Synthesis and characterization of sodium-titanium phosphates, $Na_4(TiO)(PO_4)_2$, $Na(TiO)PO_4$, and $NaTi_2(PO_4)_3$, J. Solid State Chem. 73 (1988) 317–324, doi:10.1016/0022-4596(88)90115-6.

[62] S. Benmokhtar, H. Belmal, A. El Jazouli, J.P. Chaminade, P. Gravereau, S. Pechev, J.C. Grenier, G. Villeneuve, D. de Waal, Synthesis, structure, and physicochemical investigations of the new α $Cu_{0.50}TiO(PO_4)$ oxyphosphate, J. Solid State Chem. 180 (2007) 772–779, doi:10.1016/j.jssc.2006.10.040.

[63] M. Chakir, A. El Jazouli, J.P. Chaminade, F. Bouree, D. de Waal, New process of preparation, X-ray characterisation, structure and vibrational studies of a solid solution $LiTiOAs_{1-x}P_xO_4$ ($0 \leqslant x \leqslant 1$), J. Solid State Chem. 179 (2006) 18–28, doi:10.1016/j.jssc.2005.09.047.

[64] A.F.L. Almeida, P.B.A. Fechine, J.M. Sasaki, A.P. Ayala, J.C. Góes, D.L. Pontes, W. Margulis, A.S.B. Sombra, Optical and electrical properties of barium titanate-hydroxyapatite composite screen-printed thick films, Solid State Sci.. 6(3), 267–278. doi:10.1016/j.solidstatesciences.2003.12.010.

[65] N. Anantharamulu, K.K. Rao, M. Vithal, G. Prasad, Preparation, characterization, impedance and thermal expansion studies of $Mn_{0.50}MSb(PO_4)_3$, (M = Al, Fe and Cr), J. Alloys Compd. 479 (2009) 684–691, doi:10.1016/j.jallcom.2009.01.038.

[66] R. Hepzi Pramila Devamani, M. Alagar, Synthesis and characterization of aluminium phosphate nanoparticles, Int. J. Appl. Eng. 1 (2012) 769–775, doi:10.6088/ijaser.0020101078.
[67] Y. Iida, K. Sawamura, K. Iwasaki, T. Nakanishi, F. Iwakura, Y. Nakajima, A. Yasumori, Persistent luminescence properties of Ti^{4+}-doped $K_2ZrSi_3O_9$ wadeite, Sensors Mater. 32 (4) (2020) 1427–1433, doi:10.18494/SAM.2020.2745.
[68] X. Meng, S. Murai, K. Fujita, K. Tanaka, Intense visible emission from d^0 ions-doped silicate glasses, J. Ceram. Soc. Japan. 116 (10) (2008) 1147–1149, doi:10.2109/jcersj2.116.1147.
[69] S. Benmokhtar, A. El Jazouli, S. Krimi, J.P. Chaminade, P. Gravereau, M. Menetrier, D. de Waal, Synthesis, structure refinement and characterisation of a new oxyphosphate $Mg_{0.50}TiO(PO_4)$, Mater. Res. Bull. 42 (5) (2007) 892–903, doi:10.1016/j.materresbull.2006.08.020.